Analysis of drag reduction by polymers in a turbulent channel flow

By B. K. Lieu† AND M. R. Jovanović†

We develop a model-based approach for studying the influence of polymers on drag reduction in a turbulent channel flow. Our simulation-free method utilizes turbulence modeling in conjunction with the analysis of stochastically forced linearized equations to capture the effect of velocity and polymer stress fluctuations on the turbulent viscosity and drag. We demonstrate that the essential drag-reducing trends observed in direct numerical simulations are captured by our approach.

1. Introduction

The addition of a small amount of polymers to turbulent flows is an effective means for reducing skin-friction losses (White & Mungal 2008). Most of our understanding of the onset of drag reduction and the interaction of polymers with turbulence comes from numerical and experimental studies. In particular, direct numerical simulations (DNS) have offered tremendous insight on drag reduction mechanisms (Dimitropoulos *et al.* 1998; Min *et al.* 2003), maximum drag reduction (Li *et al.* 2006; Xi & Graham 2010), and coherent structures (Dubief *et al.* 2004; Dimitropoulos *et al.* 2005; Li & Graham 2007). In spite of this success, there is a need for the development of computationally attractive models that are suitable for analysis and identification of key physical mechanisms.

In this paper, we combine turbulence modeling with analysis of stochastically forced linearized flow equations to quantify the polymer-induced drag reduction in a simulation-free manner. Our approach builds on recent efforts to develop model-based techniques for controlling the onset of turbulence (Moarref & Jovanović 2010; Lieu, Moarref & Jovanović 2010) and fully developed turbulent flows (Moarref & Jovanović 2012). In contrast to the traditional approach that relies on numerical simulations, we use eddy-viscosity-enhanced linearization to determine the influence of polymer additives on drag reduction. Our predictions capture the essential trends observed in DNS studies.

Our report is organized as follows. In Section 2, we formulate the problem and briefly discuss the governing equations and turbulence modeling. In Section 3, we examine the influence of fluctuations on the turbulent viscosity and drag using a stochastically forced model linearized around an approximation of the turbulent mean profile. We also present an efficient method for computing the second-order statistics of velocity and polymer stress fluctuations. In Section 4, we demonstrate that our model-based method is capable of predicting the essential drag-reducing trends. We conclude with a brief summary of our developments and outlook for future research in Section 5.

2. Problem formulation

We study a pressure-driven turbulent channel flow of a viscoelastic fluid in a Cartesian coordinate system (x, y, z) where x is the streamwise, y the wall-normal, and z the

† Department of Electrical and Computer Engineering, University of Minnesota, Minneapolis, MN 55455, USA.

spanwise direction. The conservation equations for momentum and mass are given by

$$\begin{aligned} \mathcal{U}_t &= -(\mathcal{U}\cdot\boldsymbol{\nabla})\mathcal{U} - \boldsymbol{\nabla}\mathcal{P} + \frac{\beta}{R_\tau}\Delta\mathcal{U} + \frac{(1-\beta)}{R_\tau}\boldsymbol{\nabla}\cdot\mathcal{T}, \\ 0 &= \boldsymbol{\nabla}\cdot\mathcal{U}, \end{aligned} \tag{2.1}$$

where $\mathcal{U}$ is the velocity vector, $\mathcal{P}$ is the pressure, $\mathcal{T}$ is the polymer stress tensor, $\boldsymbol{\nabla}$ is the gradient, and $\Delta = \boldsymbol{\nabla}\cdot\boldsymbol{\nabla}$ is the Laplacian. The Reynolds number $R_\tau = u_\tau h/\nu_0$ is defined in terms of the channel's half-height h, the friction velocity $u_\tau = \sqrt{(\tau_w/\rho)}$, and the zero shear rate kinematic viscosity $\nu_0 = \eta_0/\rho$. Here, τ_w is the wall-shear stress, ρ is the fluid density, $\eta_0 = \eta_s + \eta_p$ is the total viscosity, while η_s and η_p are the solvent and polymer viscosities. The parameter $\beta = \eta_s/\eta_0$ is the ratio of the solvent viscosity to the total viscosity; for $\beta = 1$ the fluid is Newtonian and (2.1) simplifies to the standard Navier-Stokes (NS) equations. Equations (2.1) have been brought to non-dimensional form by scaling length with h, velocity with u_τ, time with h/u_τ, pressure with τ_w, and polymer stress with $\eta_p u_\tau/h$.

We describe the evolution of the polymer stress tensor $\boldsymbol{\tau}$ using the Oldroyd-B model (Bird *et al.* 1987),

$$\mathcal{T}_t = \frac{1}{We}\Big(\boldsymbol{\nabla}\mathcal{U} + (\boldsymbol{\nabla}\mathcal{U})^T - \mathcal{T}\Big) + \mathcal{T}\cdot\boldsymbol{\nabla}\mathcal{U} + (\boldsymbol{\nabla}\mathcal{U})^T\cdot\mathcal{T} - (\mathcal{U}\cdot\boldsymbol{\nabla})\mathcal{T} + \frac{D_0}{R_\tau}\Delta\mathcal{T}. \tag{2.2}$$

The dimensionless parameter $We = \lambda u_\tau/h$ in (2.2) denotes the Weissenberg number which is defined as the ratio of the polymer relaxation time λ to the characteristic flow time h/u_τ. In turbulent flows, the friction Weissenberg number $We_\tau = \lambda u_\tau^2/\nu_0$ is typically used and the relationship between We and We_τ is given by (Housiadas & Beris 2004)

$$We = We_\tau/R_\tau.$$

The last term in (2.2) represents an artificial stress diffusive term. The numerical diffusivity is denoted by $D_0 = \kappa/\nu_0$ where κ is the isotropic numerical diffusivity. The addition of this term helps alleviate numerical instabilities associated with the standard Oldroyd-B model. For small D_0, Sureshkumar & Beris (1995) show that artificial stress diffusivity has weak influence on the flow dynamics. In DNS of turbulent channel flows, D_0 is typically chosen to have the smallest value that provides numerically stable computations.

2.1. *Equations for mean flow*

Here, we present a method for computing an approximation of the mean turbulent velocity and polymer stresses. Even though this mean flow analysis shows that polymers reduce drag, it does not capture the essential drag-reducing trends observed in DNS. In Section 3, we show that analysis of the dynamics of flow fluctuations around this approximate mean flow improves predictive capability of our model-based approach.

The mean flow equations are obtained by splitting the flow quantities into their mean and fluctuating components

$$\mathcal{U} = \mathbf{U} + \mathbf{u}, \quad \mathcal{T} = \mathbf{T} + \boldsymbol{\tau}, \quad \mathcal{P} = P + p, \tag{2.3}$$

where $\mathbf{U} = \overline{\mathcal{U}}$, $\overline{\mathbf{u}} = 0$, with the bar denoting averaging in time and horizontal directions. Substituting (2.3) into (2.1) and (2.2) and taking the average in time and horizontal directions yields the steady-state mean equations for $\mathbf{U}$ and $\mathbf{T}$ (McComb 1991; Durbin

& Reif 2000)

$$0 \;=\; -\left(\mathbf{U}\cdot\boldsymbol{\nabla}\right)\mathbf{U} \;-\; \nabla P \;+\; \frac{\beta}{R_\tau}\,\Delta\mathbf{U} \;+\; \frac{(1-\beta)}{R_\tau}\,\boldsymbol{\nabla}\cdot\mathbf{T} \;-\; \boldsymbol{\nabla}\cdot\left(\overline{\mathbf{u}\mathbf{u}^T}\right), \tag{2.4a}$$

$$0 \;=\; \boldsymbol{\nabla}\cdot\mathbf{U}, \tag{2.4b}$$

$$0 \;=\; \frac{1}{We}\left(\boldsymbol{\nabla}\mathbf{U} \;+\; \left(\boldsymbol{\nabla}\mathbf{U}\right)^T \;-\; \mathbf{T}\right) \;+\; \mathbf{T}\cdot\boldsymbol{\nabla}\mathbf{U} \;+\; \left(\boldsymbol{\nabla}\mathbf{U}\right)^T\cdot\mathbf{T} \;-\; \left(\mathbf{U}\cdot\boldsymbol{\nabla}\right)\mathbf{T} \tag{2.4c}$$

$$+\; \frac{D_0}{R_\tau}\,\Delta\mathbf{T} \;-\; \overline{\left(\mathbf{u}\cdot\boldsymbol{\nabla}\right)\boldsymbol{\tau}} \;+\; \overline{\boldsymbol{\tau}\cdot\boldsymbol{\nabla}\mathbf{u} \;+\; \left(\boldsymbol{\nabla}\mathbf{u}\right)^T\cdot\boldsymbol{\tau}}.$$

Since the second-order statistics of the fluctuations are not known *a priori*, system (2.4) exhibits a closure problem. The first unknown term is the Reynolds stress tensor, $\overline{\mathbf{u}\mathbf{u}^T}$, which quantifies the transport of momentum arising from turbulent fluctuations (McComb 1991). The remaining terms appear in the mean constitutive equation (2.4c),

$$\Gamma \;=\; \overline{\left(\mathbf{u}\cdot\boldsymbol{\nabla}\right)\boldsymbol{\tau}}, \quad \Lambda \;=\; \overline{\boldsymbol{\tau}\cdot\left(\boldsymbol{\nabla}\mathbf{u}\right) \;+\; \left(\boldsymbol{\nabla}\mathbf{u}\right)^T\cdot\boldsymbol{\tau}}, \tag{2.5}$$

where Γ represents the contribution to the transport of the polymer stress tensor arising from the fluctuating advective terms, and Λ accounts for the interactions between the fluctuating components of the polymer stress tensor and the velocity gradient tensor.

2.2. *Turbulent eddy viscosity*

One of the most commonly used models for the second-order statistics of velocity fluctuations is the Boussinesq approximation (McComb 1991)

$$\overline{\mathbf{u}\mathbf{u}^T} \;=\; \frac{2}{3}\,k\,I \;-\; \frac{\beta\,\nu_T}{R_\tau}\left(\boldsymbol{\nabla}\mathbf{U} \;+\; \left(\boldsymbol{\nabla}\mathbf{U}\right)^T\right), \tag{2.6}$$

where k is the turbulent kinetic energy, I is the identity operator, and ν_T is the turbulent eddy viscosity. In turbulent flows of viscoelastic fluids, ν_T is determined from statistics of velocity fluctuations and it is not known *a priori*. Hence, in order to accurately capture influence of velocity fluctuations on the turbulent mean velocity and polymer stresses we need an accurate model of ν_T. For a turbulent channel flow of Newtonian fluids, Reynolds & Tiederman (1967) proposed the following model for the turbulent eddy viscosity

$$\nu_{T0}(y) \;=\; \frac{1}{2}\left(\left(1 \;+\; \left(\frac{c_2}{3}\,R_\tau\,(1-y^2)\,(1+2y^2)\,\left(1-e^{-(1-|y|)\,R_\tau/c_1}\right)\right)^2\right)^{1/2} - 1\right), \tag{2.7}$$

where c_1 and c_2 are modeling parameters selected to minimize least squares deviation between the mean streamwise velocity obtained with turbulent viscosity (2.7), and the mean streamwise velocity obtained in experiments and simulations. In particular, for DNS data of Del Alamo & Jiménez (2003) at $R_\tau = 186$ we have $\{c_1 = 0.61, c_2 = 46.2\}$.

For flow subject to a constant pressure gradient $P_x = -1$, we determine an approximation to the mean turbulent profiles by neglecting the influence of fluctuations (2.5) in (2.4c) and utilizing (2.6) with eddy viscosity profile (2.7),

$$\mathbf{U} \;=\; \begin{bmatrix} U(y) \\ 0 \\ 0 \end{bmatrix}, \quad \mathbf{T} \;=\; \begin{bmatrix} T_{11}(y) & T_{12}(y) & 0 \\ T_{12}(y) & 0 & 0 \\ 0 & 0 & 0 \end{bmatrix}.$$

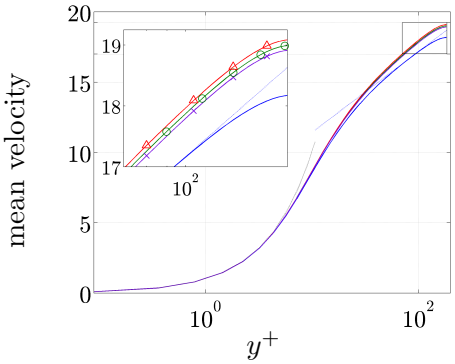

FIGURE 1. Mean velocity as a function of the distance from the wall in flows with no polymers $U_0(y^+)$ (solid); and with polymers $U(y^+)$ for $We_\tau = 10$ ($\triangle$), $We_\tau = 50$ ($\circ$), and $We_\tau = 100$ ($\times$). For Newtonian fluids, we also show the linear wall asymptote, $U = y^+$, and the logarithmic inertial sublayer asymptote, $U = 2.5\ln(y^+) + 6.5$. Results are obtained for flows with $R_\tau = 186$, $\beta = 0.9$, and $D_0 = 3.25$ using approximation up to fifth-order in α and the assumption that turbulent viscosity ν_{T0} captures the behavior of fluctuations.

Homogeneous Dirichlet boundary conditions are imposed on U, and the boundary conditions for the polymer stresses are obtained using the procedure described in Sureshkumar & Beris (1995).

We next utilize perturbation analysis with $\alpha = 1 - \beta$ as the perturbation parameter to represent non-zero components of $\mathbf{U}$ and $\mathbf{T}$ as

$$\begin{aligned} U(y) &= U_0(y) + \alpha\, U_1(y) + \alpha^2\, U_2(y) + \mathcal{O}(\alpha^3), \\ T_{1j}(y) &= T_{1j,0}(y) + \alpha\, T_{1j,1}(y) + \alpha^2\, T_{1j,2}(y) + \mathcal{O}(\alpha^3), \quad j = \{1, 2\}. \end{aligned}$$

By construction, U_0 approximates the mean streamwise velocity in the turbulent flow of Newtonian fluids. On the other hand, U_i, $T_{11,i}$, and $T_{12,i}$ for $i = 1, 2, \ldots$, denote corrections to U_0, $T_{11,0}$, and $T_{12,0}$ induced by polymers. They are obtained under the assumption that the turbulent viscosity is not modified by polymers and that the second-order statistics of fluctuations do not influence the mean polymer stresses. Figure 1 shows the turbulent mean velocity profiles for the flow with no polymers U_0 and for the flow with polymers U as a function of the distance from the wall, $y^+ = R_\tau\,(y + 1)$.

As shown in Figure 1, the linear relationship $U = y^+$ is satisfied in the viscous sublayer close to the wall ($y^+ < 2$). In the inertial sublayer far away from the wall ($y^+ > 50$), the Newtonian turbulent mean velocity is approximated by the logarithmic profile $U = 2.5\ln(y^+) + 6.5$. This indicates that the turbulent mean profile computed using turbulent viscosity (2.7) captures the essential trends in turbulent flows with no polymers. In flows with polymers, U is increased in the inertial sublayer and the amount of increase is reduced as We_τ increases. Note that the convergence of the perturbation series for the mean velocity and polymer stresses is verified by full-scale nonlinear computations.

In flows with polymers, Housiadas & Beris (2004) defined drag reduction as

$$DR \;=\; 1 \,-\, \left(U_B/U_{B,0}\right)^{-2/n}, \;\; n \;=\; 1.14775, \tag{2.8}$$

where U_B and $U_{B,0}$ denote bulk velocities of flows with and without polymers,

$$U_B \;=\; \int_{-1}^{1} U(y)\,\mathrm{d}y.$$

The mean velocity profiles shown in Figure 1 induce 7.27%, 6.75%, and 5.77% of drag reduction at $We_\tau = 10$, 50, and 100, respectively. Although in all three cases drag reduction is achieved, decrease in drag reduction with We_τ contradicts DNS trends (Sureshkumar *et al.* 1997). This indicates that the amount of drag reduction at large values of We_τ is not correctly predicted by the above mean flow analysis. In what follows, we show that dynamics of velocity and polymer stress fluctuations around the aforementioned mean profiles play a crucial role in predicting the correct polymer drag reducing trends.

3. Stochastically forced flow with polymers: fluctuation dynamics

In this section, we examine the dynamics of infinitesimal velocity and polymer stress fluctuations around the mean flow $(\mathbf{U}, \mathbf{T})$ of Section 2.2. Our model-based approach is similar to the method that Moarref & Jovanović (2012) recently used to design drag-reducing transverse wall-oscillations. Our analysis utilizes the NS and constitutive equations linearized around the turbulent mean flow of Section 2.2

$$\begin{aligned}
\mathbf{u}_t \;=\; & -(\mathbf{U}\cdot\boldsymbol{\nabla})\,\mathbf{u} - (\mathbf{u}\cdot\boldsymbol{\nabla})\,\mathbf{U} - \nabla p + \\
& \frac{1-\alpha}{R_\tau}\,\boldsymbol{\nabla}\cdot\left((1+\nu_{T0})\left(\boldsymbol{\nabla}\mathbf{u} + (\boldsymbol{\nabla}\mathbf{u})^T\right)\right) + \frac{\alpha}{R_\tau}\,\boldsymbol{\nabla}\cdot\boldsymbol{\tau}, && (3.1a)\\
0 \;=\; & \boldsymbol{\nabla}\cdot\mathbf{u}, && (3.1b)\\
\boldsymbol{\tau}_t \;=\; & \frac{1}{We}\left(\boldsymbol{\nabla}\mathbf{u} + (\boldsymbol{\nabla}\mathbf{u})^T - \boldsymbol{\tau}\right) + \frac{D_0}{R_\tau}\,\Delta\boldsymbol{\tau} + && (3.1c)\\
& \mathbf{T}\cdot\boldsymbol{\nabla}\mathbf{u} + (\boldsymbol{\nabla}\mathbf{u})^T\cdot\mathbf{T} - (\mathbf{u}\cdot\boldsymbol{\nabla})\,\mathbf{T} + \boldsymbol{\tau}\cdot\boldsymbol{\nabla}\mathbf{U} + (\boldsymbol{\nabla}\mathbf{U})^T\cdot\boldsymbol{\tau} - (\mathbf{U}\cdot\boldsymbol{\nabla})\,\boldsymbol{\tau},
\end{aligned}$$

where $\alpha = 1-\beta$ and

$$\mathbf{u} \;=\; \begin{bmatrix} u \\ v \\ w \end{bmatrix}, \quad \boldsymbol{\tau} \;=\; \begin{bmatrix} \tau_{11} & \tau_{12} & \tau_{13} \\ \tau_{12} & \tau_{22} & \tau_{23} \\ \tau_{13} & \tau_{23} & \tau_{33} \end{bmatrix}.$$

The evolution form of (3.1) is obtained by eliminating the pressure from the equations, and by expressing the velocity fluctuations in terms of the wall-normal velocity v and vorticity $\eta = \partial_z u - \partial_x w$. Furthermore, by rearranging the components of $\boldsymbol{\tau}$ and by applying the Fourier transforms in the x and z-directions, we arrive at a set of partial differential equations in y and t parameterized by the wave-numbers $\boldsymbol{\kappa} = (k_x, k_z)$,

$$\begin{aligned}
\boldsymbol{\psi}_t(y,\boldsymbol{\kappa},t) \;&=\; A(\boldsymbol{\kappa})\,\boldsymbol{\psi}(y,\boldsymbol{\kappa},t) + B(\boldsymbol{\kappa})\,\mathbf{f}(y,\boldsymbol{\kappa},t),\\
\boldsymbol{\phi}(y,\boldsymbol{\kappa},t) \;&=\; C(\boldsymbol{\kappa})\,\boldsymbol{\psi}(y,\boldsymbol{\kappa},t),
\end{aligned} \qquad (3.2)$$

where $\boldsymbol{\psi} = \begin{bmatrix} \boldsymbol{\psi}_1^T & \boldsymbol{\psi}_2^T \end{bmatrix}^T$ is the state vector with

$$\boldsymbol{\psi}_1 = \begin{bmatrix} v & \eta \end{bmatrix}^T, \quad \boldsymbol{\psi}_2 = \begin{bmatrix} \tau_{22} & \tau_{23} & \tau_{33} & \tau_{12} & \tau_{13} & \tau_{11} \end{bmatrix}^T.$$

The output vector $\boldsymbol{\phi}$ contains the velocity and polymer stress fluctuations. Due to space constraints, the operators in (3.2) will be reported elsewhere. System (3.2) is forced with a zero-mean temporally white stochastic process $\mathbf{f}$,

$$\mathcal{E}\left(\mathbf{f}(\cdot,\boldsymbol{\kappa},t_1)\otimes\mathbf{f}(\cdot,\boldsymbol{\kappa},t_2)\right) \;=\; M(\boldsymbol{\kappa})\,\delta(t_1 - t_2), \qquad (3.3)$$

where δ is the Dirac delta function, $\mathbf{f}\otimes\mathbf{f}$ is the tensor product of $\mathbf{f}$ with itself, and $M(\boldsymbol{\kappa})$ is the spatial spectral-density of the forcing.

Jovanović & Georgiou (2010) showed that the steady-state statistics of velocity fluctuations in homogeneous isotropic turbulence can be reproduced by driving linearized NS equations with white-in-time forcing and properly selected spatial spectral-density. Inspired by this observation, Moarref & Jovanović (2012) determined $M(\boldsymbol{\kappa})$ to match the DNS-generated energy spectrum in Newtonian turbulent channel flows. We adopt the model for spatial spectral-density of forcing developed in Moarref & Jovanović (2012).

For the linearized system (3.2), the steady-state autocorrelation tensor of flow fluctuations is obtained by solving the Lyapunov equation (Jovanović & Bamieh 2005)

$$A(\boldsymbol{\kappa})\, X(\boldsymbol{\kappa}) \,+\, X(\boldsymbol{\kappa})\, A^*(\boldsymbol{\kappa}) \;=\; -B(\boldsymbol{\kappa})\, M(\boldsymbol{\kappa})\, B^*(\boldsymbol{\kappa}), \tag{3.4}$$

where the asterisk denotes the adjoint of the corresponding operator. The operator X represents the autocorrelation operator of $\boldsymbol{\psi}$ and it contains all second-order statistics of velocity and polymer stress fluctuations. Furthermore, since we use a perturbation series to represent the mean velocity $\mathbf{U}$, the operator X can be represented as

$$X \;=\; X_0 \,+\, \alpha\, X_1 \,+\, \alpha^2\, X_2 \,+\, \mathcal{O}(\alpha^3), \tag{3.5}$$

where X_0 denotes the autocorrelation operator in the turbulent flow of Newtonian fluids, and X_i for $i = \{1, 2, 3, \ldots\}$ denote the corrections induced by polymers.

By selecting proper velocity and length scales, the eddy viscosity can be expressed as (McComb 1991)

$$\nu_T \;=\; C_\mu\, R_\tau^2\, \left(k^2/\epsilon\right), \tag{3.6}$$

where ϵ is the rate of energy dissipation and $C_\mu = 0.09$ is a model constant. Here, we utilize the autocorrelation operator X to determine the second-order statistics of the velocity fluctuations and consequently k and ϵ. By expressing k and ϵ in terms of power series expansion (in α), ν_T can be represented as

$$\nu_T \;=\; \nu_{T0} \,+\, \alpha\, \nu_{T1} \,+\, \mathcal{O}(\alpha^3), \quad \nu_{T1} \;=\; \nu_{T0}\, (2\, k_1/k_0 \,-\, \epsilon_1/\epsilon_0), \tag{3.7}$$

where ν_{T0} is the Reynolds–Tiederman eddy viscosity profile (2.7).

The developments of this section are used to study the influence of polymers on the turbulent viscosity, mean velocity, drag, and turbulent kinetic energy; see Section 4 for details.

4. Results and discussion

In this section, we examine the effect of flow fluctuations on the eddy viscosity, turbulent mean velocity, drag and turbulent kinetic energy in flows with $R_\tau = 186$, $\beta = 0.9$ and $D_0 = 3.25$. We also analyze how We_τ influences the drag reduction and compare our predictions with DNS results of Li *et al.* (2006). Furthermore, we study how polymers influence the energy amplification of turbulent velocity fluctuations.

We use perturbation analysis up to fifth order in α for all our computations. In addition, for each computed flow quantity a series acceleration method known as Shanks transformation (Shanks 1955) is used to increase the rate of convergence of the perturbation series. The finite-dimensional approximations of the underlying operators are obtained using the pseudospectral method (Weideman & Reddy 2000). An automatic Chebyshev collocation method (Trefethen *et al.* 2011) was also employed to verify our results.

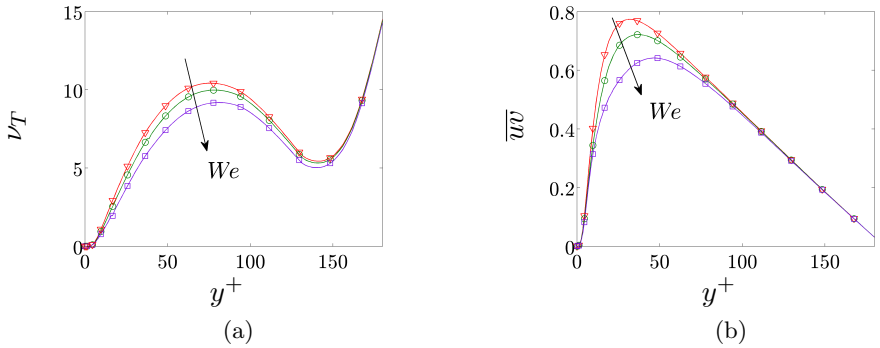

FIGURE 2. (a) Turbulent eddy viscosity ν_T and (b) Reynolds stress $\overline{uv}$ as a function of y^+ for $R_\tau = 186$, $\beta = 0.9$, $D_0 = 3.25$: $We_\tau = 50$ ($\triangledown$); $We_\tau = 70$ ($\circ$); and $We_\tau = 100$ ($\square$). Perturbation series up to fifth order in α with Shanks approximation is used to obtain ν_T and $\overline{uv}$.

4.1. *Turbulent eddy viscosity and Reynolds shear stress*

We first discuss the effect of polymers on the turbulent eddy viscosity ν_T and Reynolds shear stress $\overline{uv}$. Figure 2(a) shows the turbulent viscosity ν_T obtained using (3.6). The eddy viscosity increases from zero at the channel wall to a maximum value within the core of channel. As the friction Weissenberg number increases, ν_T decreases at all points in the channel. In flows with polymers, the Reynolds shear stress shown in Figure 2(b) is computed using the second-order statistics of stochastically forced linearized equations. Similar to the eddy viscosity, the value of $\overline{uv}$ decreases throughout the channel as We_τ increases. We note that reductions in the turbulent eddy viscosity and Reynolds shear stress indicate that the drag is reduced; see Section 4.2 for additional details. Furthermore, the above-observed trends are in good agreement with the numerical findings of Li *et al.* (2006) and Iaccarino *et al.* (2010).

4.2. *Turbulent mean velocity and drag reduction*

We next examine the influence of velocity and polymer stress fluctuations on the streamwise mean velocity and drag reduction. The modified turbulent mean velocity and polymer stresses are obtained by solving the equations for mean flow (2.4) – (2.6) with the corrected eddy viscosity (3.6). Note that the second-order statistics of flow fluctuations (2.5), Γ and Λ, are obtained from the autocorrelation operator, X.

The modified turbulent mean velocity and drag reduction are shown in Figure 3. Figure 3(a) demonstrates that the fluctuations around the base flow computed in Section 2.2 have profound influence on the turbulent mean flow; c.f. Figures 1 and 3(a). For all mean velocities, the constant pressure gradient constraint induces a linear dependence on y^+ in the viscous sublayer close to the wall. As the friction Weissenberg number We_τ increases, the streamwise velocity is increased in the inertial sublayer, which also increases the amount of drag reduction; see Figure 3(b). Figure 3(b) also shows a curve that provides a best fit to the amount of drag reduction obtained in simulations of the FENE-P model (Li *et al.* 2006). Although the amount of drag reduction computed using our simulation-free method does not match exactly the fitted curve, the drag-reducing trends as a function of We_τ are nicely captured. More interestingly, it appears that our method is capable of capturing the saturation of drag reduction at large We_τ. This phenomenon is known as the maximum drag reduction asymptote (White & Mungal 2008). In our

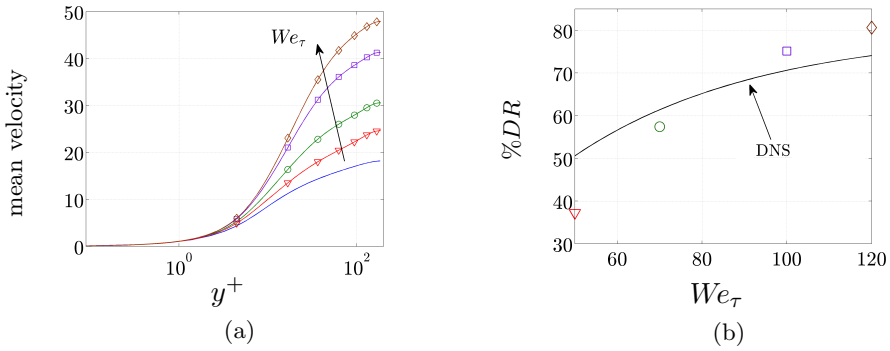

FIGURE 3. Modified turbulent mean streamwise velocity and drag reduction computed using ν_T, Γ and Λ for $R_\tau = 186$, $\beta = 0.9$ and $D_0 = 3.25$. (a) streamwise mean velocity as a function of the distance from the wall, $y^+ = R_\tau\,(y+1)$: with no polymers U_0 (solid); and with polymers U for $We_\tau = 50$ ($\triangledown$), $We_\tau = 70$ ($\circ$), $We_\tau = 100$ ($\square$) and $We_\tau = 120$ ($\diamond$). (b) Drag reduction obtained using the mean velocities shown in (a). An approximation of the amount of drag reduction achieved in high-fidelity simulations of Li *et al.* (2006) is also shown (solid line) in (b).

future work, we intend to gain additional insight into this phenomenon by conducting study of the drag reduction dependence on $1/We_\tau$ in flows with high We_τ.

4.3. *Turbulent kinetic energy*

Here, we study the energy amplification of velocity fluctuations in the flow with polymers. Up to the second order in α, we have

$$\begin{aligned} E(k_x,k_z) &= E_0(k_x,k_z) + \alpha\, E_1(k_x,k_z) + \alpha^2\, E_2(k_x,k_z) + \mathcal{O}\left(\alpha^3\right), \\ &= E_0(k_x,k_z) + E_p(k_x,k_z), \end{aligned}$$

where E_0 represents the energy spectrum of the flow with no polymers and E_p denotes the correction induced by polymers. The energy spectrum of the turbulent channel flow of Newtonian fluids E_0 is obtained by Del Alamo & Jiménez (2003) and it is always positive. On the other hand, the corrections to it can assume both positive and negative values. Figure 4 shows the corrections to the pre-multiplied energy spectrum of the velocity fluctuations induced by polymers, $\mathcal{E}_p(k_x,k_z) = k_x\, k_z\, E_p(k_x,k_z)$.

In all three cases, the integral of $\mathcal{E}_p$ is positive indicating that polymer additives increase the turbulent kinetic energy, which is in agreement with the DNS results of Min *et al.* (2003). At $We_\tau = 50$, Figure 4(a) shows energy amplification in the region where $k_x \sim \mathcal{O}(1)$ and $k_z \sim \mathcal{O}(1)$. As the Weissenberg number increases, the largest amplification decreases. Furthermore, in all three cases, there is a narrow region of wavenumbers where polymers slightly reduce fluctuations' energy; as We_τ increases, the amplitude in this region gets increased. This illustrates that energy amplification is reduced as the ratio of the polymer relaxation time to the characteristic flow time increases. We note that further investigation into the kinetic energy equation may provide additional insight into the mechanisms behind energy amplification in flows with polymers.

5. Concluding remarks

We have developed a model-based approach for studying polymer drag reduction in a turbulent channel flow. Our simulation-free method provides a computationally-efficient way for predicting the amount of drag reduction by polymer additives. This is achieved

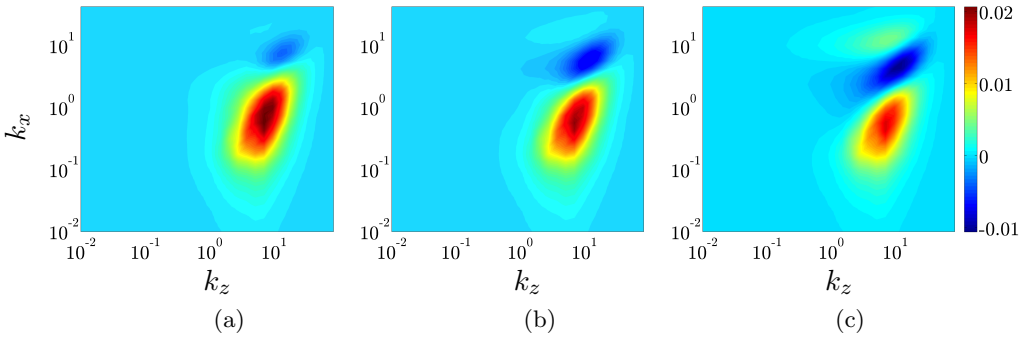

FIGURE 4. Corrections to the pre-multiplied energy spectrum of velocity fluctuations induced by polymers, $\mathcal{E}_p(k_x, k_z) = k_x\, k_z\, E_p(k_x, k_z)$, for $R_\tau = 186$, $\beta = 0.9$, and $D_0 = 3.25$: (a) $We_\tau = 50$; (b) $We_\tau = 70$; and (c) $We_\tau = 100$. Perturbation series up to fifth order in α are used with Shanks approximation. All figures are shown in log-log-lin scale.

by combining a turbulent viscosity hypothesis with stochastically forced linearized flow equations to study the influence of infinitesimal fluctuations around the turbulent mean flow with polymers on drag reduction. The predicted turbulent mean velocity and drag reduction trends agree with previously reported DNS results. Furthermore, we have identified the spatial length scales of the fluctuations that are most amplified by stochastic disturbances.

Our results illustrate the predictive power of our model-based method and set the stage for studying the physical mechanisms responsible for both the onset of drag reduction and the maximum drag reduction asymptote. Our ongoing effort is dedicated to identifying the underlying physics in the high Weissenberg number regime.

Acknowledgements

Part of this work was performed during the 2012 CTR Summer Program with financial support from Stanford University and NASA Ames Research Center. We would like to thank Prof. P. Moin for his interest in our work and for providing us with the opportunity to participate in the CTR Summer Program; and to Dr. J. W. Nichols for his useful comments that helped us improve quality of our paper. Financial support from the National Science Foundation under CAREER Award CMMI-06-44793 is gratefully acknowledged. The University of Minnesota Supercomputing Institute is acknowledged for providing computing resources.

REFERENCES

BIRD, R. B., CURTISS, C. F., ARMSTRONG, R. C. & HASSAGER, O. 1987 *Dynamics of Polymeric Fluids*. Wiley.

DEL ALAMO, J. C. & JIMÉNEZ, J. 2003 Spectra of the very large anisotropic scales in turbulent channels. *Phys. Fluids* **15** (6), 41–44.

DIMITROPOULOS, C. D., DUBIEF, Y., SHAQFEH, E. S. G., MOIN, P. & LELE, S. K. 2005 Direct numerical simulation of polymer-induced drag reduction in turbulent boundary layer flow. *Phys. Fluids* **17**, 011705.

DIMITROPOULOS, C. D., SURESHKUMAR, R. & BERIS, A. N. 1998 Direct numerical simulation of viscoelastic turbulent channel flow exhibiting drag reduction: effect of the variation of rheological parameters. *J. Non-Newtonian Fluid Mech.* **79**, 433–468.

Dubief, Y., White, C. M., Terrapon, V. E., Shaqfeh, E. S. G., Moin, P. & Lele, S. K. 2004 On the coherent drag-reducing and turbulence-enhancing behaviour of polymers in wall flows. *J. Fluid Mech.* **514**, 271–280.

Durbin, P. A. & Reif, B. A. P. 2000 *Theory and Modeling of Turbulent Flows*. Wiley.

Housiadas, K. D. & Beris, A. N. 2004 An efficient fully implicit spectral scheme for DNS of turbulent viscoelastic channel flow. *J. Non-Newtonian Fluid Mech.* **122**, 243–262.

Iaccarino, G., Shaqfeh, E. S. G. & Dubief, Y. 2010 Reynolds-averaged modeling of polymer drag reduction in turbulent flows. *J. Non-Newtonian Fluid Mech.* **165**, 376–384.

Jovanović, M. R. & Bamieh, B. 2005 Componentwise energy amplification in channel flows. *J. Fluid Mech.* **534**, 145–183.

Jovanović, M. R. & Georgiou, T. T. 2010 Reproducing second order statistics of turbulent flows using linearized navier-stokes equations with forcing. *Bulletin of the American Physical Society* **55**.

Li, C. F., Gupta, V. K., Sureshkumar, R. & Khomami, B. 2006 Turbulent channel flow of dilute polymeric solutions: Drag reduction scaling and an eddy viscosity model. *J. Non-Newtonian Fluid Mech.* **139**, 177–189.

Li, W. & Graham, M. D. 2007 Polymer induced drag reduction in exact coherent structures of plane Poiseuille flow. *Phys. Fluids* **19**, 083101.

Lieu, B. K., Moarref, R. & Jovanović, M. R. 2010 Controlling the onset of turbulence by streamwise traveling waves. Part 2: Direct numerical simulations. *J. Fluid Mech.* **663**, 100–119.

McComb, W. D. 1991 *The Physics of Fluid Turbulence*. Oxford University Press.

Min, T., Yoo, J. Y., Choi, H. & Joseph, D. D. 2003 Drag reduction by polymer additives in a turbulent channel flow. *J. Fluid Mech.* **486**, 213–238.

Moarref, R. & Jovanović, M. R. 2010 Controlling the onset of turbulence by streamwise traveling waves. Part 1: Receptivity analysis. *J. Fluid Mech.* **663**, 70–99.

Moarref, R. & Jovanović, M. R. 2012 Model-based design of transverse wall oscillations for turbulent drag reduction. *J. Fluid Mech.* **707**, 205–240.

Reynolds, W. C. & Tiederman, W. G. 1967 Stability of turbulent channel flow with application to malkus's theory. *J. Fluid Mech.* **27** (2), 253–272.

Shanks, D. 1955 Nonlinear transformations of divergent and slowly convergent sequences. *J. Math. Phys.* **34**, 1–42.

Sureshkumar, R. & Beris, A. N. 1995 Effect of artificial stress diffusivity on the stability of numerical calculations and the flow dynamics of time-dependent viscoelastic flows. *J. Non-Newtonian Fluid Mech.* **60**, 53–80.

Sureshkumar, R., Beris, A. N. & Handler, R. A. 1997 Direct numerical simulation of the turbulent channel flow of a polymer solution. *Phys. Fluids* **9**, 743–755.

Trefethen, L. N., Hale, N., Platte, R. B., Driscoll, T. A. & Pachón, R. 2011 Chebfun version 4. University of Oxford, `http://www.maths.ox.ac.uk/chebfun/`.

Weideman, J. A. C. & Reddy, S. C. 2000 A MATLAB differentiation matrix suite. *ACM T. Math. Software* **26** (4), 465–519.

White, C. M. & Mungal, M. G. 2008 Mechanics and prediction of turbulent drag reduction with polymer additives. *Annu. Rev. Fluid Mech.* **40**, 235–256.

Xi, L. & Graham, M. D. 2010 Turbulent drag reduction and multistage transitions in viscoelastic minimal flow units. *J. Fluid Mech.* **647**, 421–452.